

# Modelling and Simulation of Square Diaphragm Touch Mode Capacitive Pressure Sensor (TMCPS)

Maibam Sanju Meetei, Nabam Naga, Nyari Taji and Rakesh Sharma

Rajiv Gandhi University

[maibamkhuman@gmail.com](mailto:maibamkhuman@gmail.com), [naganabam7@gmail.com](mailto:naganabam7@gmail.com), [nyaritaji5@gmail.com](mailto:nyaritaji5@gmail.com), [rakesh.tulas@gmail.com](mailto:rakesh.tulas@gmail.com)

**Abstract** - This research presents and validates a mathematical model of the TMCPS using the COMSOL Multiphysics simulator. Utilizing a novel technique, the output characteristic of TMCPS is linearized by converting the diaphragm's deflection into a linear displacement using a mechanical coupler. Using mechanical and electrostatic models, the maximum deflection of the square diaphragm and the output capacitance with its sensitivity are explored. Using a COMSOL Multiphysics simulator, a 3D model of a recommended sensor is constructed to evaluate the results of the mathematically represented equations. It is demonstrated that a number of factors affect the sensor's outputs, including the diaphragm's size and shape, Poisson's ratio, Young modulus, the type of dielectric polymer employed, the size of the capacitor plates physically, and the space between the plates. The sensitivity of the PMMA-based touch mode capacitive pressure is 0.09 fF/MPa for simulated pressure and 0.09 fF/MPa for calculated pressure for a 15  $\mu\text{m}$  thick diaphragm.

**Index Terms** - deflection, mechanical coupler, non-linear, sensitivity, TMCPS.

## INTRODUCTION

The words "Pressure" and "Sensor" are the origins of the name "Pressure Sensor." On a surface, pressure is the force per unit area. Its meter- kilogram- second (MKS) based unit is the Pascal (Pa). A sensor is an object with a sensitive component that can change a physical quantity into an electrical quantity. As a result, a pressure-sensitive element that can be converted to an electrical amount makes up a pressure sensor. In its most basic form, a pressure sensor is an instrument that transforms mechanical pressure (such as liquid or gas pressure) into an electrical amount (current, voltage or charge). Different kinds of pressure sensors have been developed, manufactured in large quantities, and sold.

Many types of pressure sensors are researched in various literatures based on their sensing processes:

- Resistive pressure sensor: a piezo-resistive pressure sensor that changes resistance as a result of deformation caused by applying pressure [1-3]. When the size of the sensor is reduced, the strain is reduced, resulting in a drop in sensitivity.
- Capacitive pressure sensor: the displacement of a diaphragm according to applied pressure affects the electrical capacitance of this sensor [3-6]. Because the capacitance of this sensor is inversely proportional to the separation of the capacitor plates, it has nonlinear properties.
- Inductive pressure sensor: this sensor operates on the concept of magnetic field induction, showing the primary scaling and magnetic interference limitations caused by metals [7-8].
- Thermal pressure sensor: this sensor works on the principle that thermal conductivity increases as density varies in response to input pressure [9-10]. The system's intricacy is the major drawback.
- Piezoelectric pressure sensor: this sensor uses piezoelectric effect to measure dynamic pressure [11-13]. The fundamental disadvantage of such a sensor is that it can only detect dynamic pressure.

A pressure sensor type with numerous uses in Micro-Electro-Mechanical Systems (MEMS) is the capacitive pressure sensor. Mutual and self-capacitance are the two categories under which capacitance is classified. This

condition involves measuring the electric potential gradient between the object and the ground in order to determine an object's self-capacitance, or ability to retain charge. Mutual capacitance results from the built-up charge between two conductors, one of which is negatively charged and the other positively charged; the electric potential between the two conductors is then determined.

Capacitive pressure sensors can be miniaturized and manufactured using MEMS technology. The capacitances of capacitive pressure sensors are determined by the capacitor structure and the dielectric material used between the plates. Planar capacitive pressure sensors, comb drive capacitive pressure sensors, and touch mode capacitive pressure sensors are the three main types of capacitive pressure sensors. In TMCPS, dielectric materials divide the moveable and non-movable plates. Touch mode gets its name from the fact that the two plates are in contact while they operate. The TMCPS output rises, when the gap between the two plates narrows due to the presence of dielectric material between the plates. As a result, TMCPS perform better than planar type and comb type capacitive pressure sensor. However, the outputs are noticeably non-linear in response to the input pressure.

### MATHEMATICAL MODELLING

It is necessary to design a mathematical sensor model and run simulations to verify its framework before developing a sensor prototype. MEMS devices contain mechanical and electrostatic modules. It is essential to use mechanical and electrostatic modelling. The pressure is applied to the sensor's diaphragm. The three most common types of diaphragms are square, circular, and rectangular. In this study takes a square diaphragm structure. The side view of a square based diaphragm TMCPS is shown in figure 1.

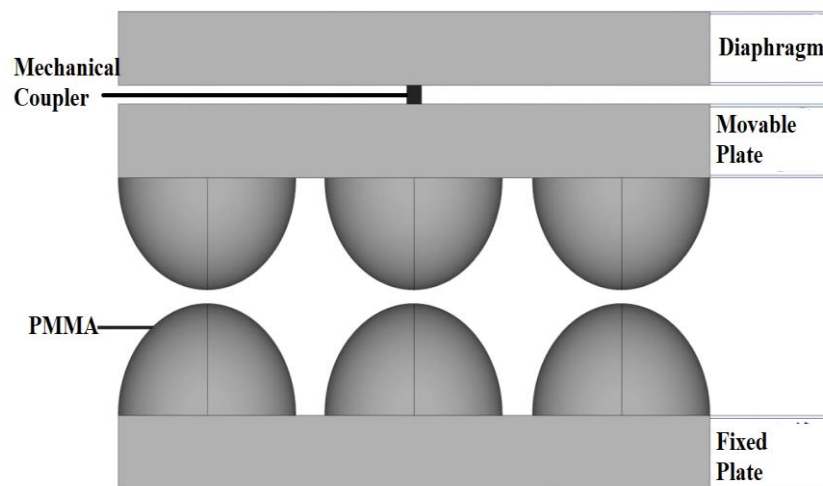


FIGURE 1

SIDE VIEW OF SQUARE BASED DIAPHRAGM TMCPS

The mechanical coupler converts the diaphragm's deflection into a linear displacement on the movable plate. The movable plate moves closer to the fixed plate as a result of the linear displacement, and the capacitance output of the sensor changes as a result of the applied pressure. The linearization of the sensor characteristic is crucially dependent on this linear displacement. The design flow of this research work is shown in figure 2.

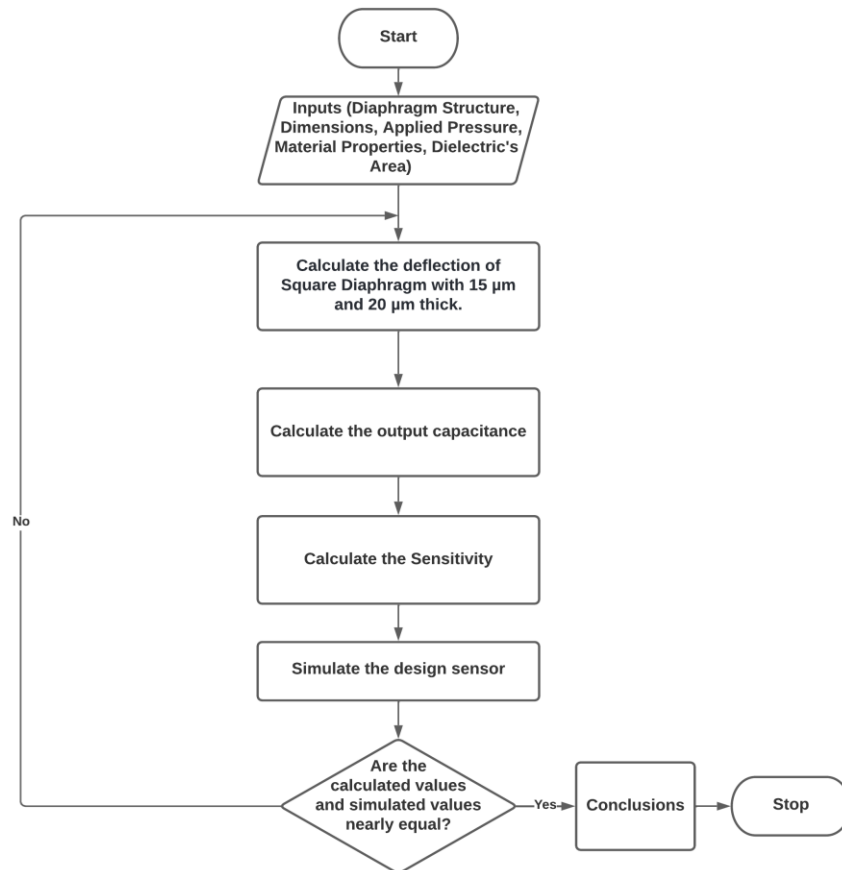


FIGURE 2  
FLOWCHART OF THE DESIGN FLOW.

### MECHANICAL MODELLING

For the same applied pressure, the square diaphragm has a higher deflection property than the other diaphragm structure, making it one of the most often used diaphragms in design. The total diaphragm energy under applied pressure is given in [14]–[16] by the rectangular diaphragm with length  $2b$  along the  $y$ -axis and breath  $2a$  along

$$U = \frac{D}{2} \int_{-b}^b \int_{-a}^a \left\{ \left( \frac{\partial^2 w}{\partial x^2} + \frac{\partial^2 w}{\partial y^2} \right)^2 - 2(1-\nu) \left[ \frac{\partial^2 w}{\partial x^2} \frac{\partial^2 w}{\partial y^2} - \left( \frac{\partial^2 w}{\partial x \partial y} \right)^2 \right] \right\} dx dy$$

the  $x$ -axis. 
$$- \int_{-b}^b \int_{-a}^a w P dx dy, \quad (1)$$

where  $U$  is the diaphragm's total energy,  $w$  is the deflection function,  $D$  is the diaphragm's flexural rigidity,  $\nu$  is the Poisson's Ratio, and  $P$  is the applied pressure.

The flexural rigidity value is calculated as follows:

$$D = \frac{Eh^3}{12(1-\nu^2)} \quad (2)$$

where  $h$  is the diaphragm thickness and  $E$  is the diaphragm material's Young's Modulus.

The displacement function of a rectangular diaphragm is given in [10-11].

$$w(x, y) = \psi (a^2 - x^2)^2 (b^2 - y^2)^2 \quad (3)$$

where  $\Psi$  is a constant.

Now, substitute equation (3) with equation (1) and impose the condition  $\frac{\partial U}{\partial \psi} = 0$ , we get

$$\psi = \frac{49P}{128(7a^4 + 4a^2b^2 + 7b^4)D} \quad (4)$$

We get by substituting equation (4) into equation (3).

$$w(x, y) = \frac{49P}{128D(7a^4 + 4a^2b^2 + 7b^4)} (a^2 - x^2)^2 (b^2 - y^2)^2 \quad (5)$$

The foregoing equation no. (5) reduces to for a square diaphragm of identical dimensions, i.e.

$$\begin{aligned} w(x, y) &= \frac{49P}{128D(7a^4 + 4a^2a^2 + 7a^4)} (a^2 - x^2)^2 (a^2 - y^2)^2, \\ &= 0.02126 \frac{Pa^4}{D} \left(1 - \frac{x^2}{a^2}\right)^2 \left(1 - \frac{y^2}{a^2}\right)^2 \end{aligned} \quad (6)$$

which denotes a square diaphragm's displacement at any given coordinates. The largest displacement occurs near the diaphragm's centre, i.e. Equation (6) is used to calculate the maximum deflection of a square diaphragm.

$$w(x, y)_{\max} = w(0, 0) = 0.02126 \frac{Pa^4}{D} \quad (7)$$

## ELECTROSTATIC MODELLING

A TMCPS with a polymer dielectric is shown in figure 1. Some of the capacitance plates are coated with hemispherical polymers, while others are not. As a result, the overall capacitance,  $C$ , is equal to the sum of capacitances  $C_1$ , which are covered by polymers, and capacitances  $C_2$ , which aren't covered by polymers. Therefore

$$C = C_1 + C_2, \quad (8)$$

Now,  $C_1$  and  $C_2$  can be expressed as

$$C_1 = n \frac{\epsilon_0 \epsilon_r}{(d - w)} \pi r^2, \quad (9)$$

$$C_2 = \frac{\epsilon_0 (A - n\pi r^2)}{(d - w)}, \quad (10)$$

where,  $\epsilon_0$  is absolute permittivity and  $\epsilon_r$  is the relative permittivity  $A$  is the dielectric material's surface area,  $d$  is the distance between the plates, and  $w$  is the diaphragm's displacement.

Therefore

$$\begin{aligned} C &= n \frac{\epsilon_0 \epsilon_r \pi r^2}{(d - w)} + \frac{\epsilon_0 (A - n\pi r^2)}{(d - w)}, \\ &= \frac{\epsilon_0 (\epsilon_r n\pi r^2 + A - n\pi r^2)}{(d - w)}, \\ &= \frac{\epsilon_0 (A + n\pi r^2 (\epsilon_r - 1))}{(d - w)}, \end{aligned} \quad (11)$$

Now the sensitivity,

$$S = \frac{\epsilon_0(A + (\epsilon_r - 1)\pi r^2)}{P(d - w)} \quad (12)$$

The dielectric constant, dielectric material radius, capacitance length and breadth, distance between plates, deflection, and absolute permittivity are now all factors that influence overall sensitivity.

### VALIDATION BY SIMULATION

A 3D model of TMCPS with a square diaphragm has a length of 300  $\mu\text{m}$  and a thickness of 15  $\mu\text{m}$  and 20  $\mu\text{m}$ , the semi spherical dielectric polymer has a radius of 40  $\mu\text{m}$ , and the square capacitor plate has a length of 300  $\mu\text{m}$  and a thickness of 20  $\mu\text{m}$ , all of which were created in the COMSOL Multiphysics simulator. The meshing size for the simulation is taken as fine. The COMSOL simulation time is depend on the meshing size and the configuration of the computer user used for simulation.

This 3D model of the sensor's structure includes a diaphragm, mechanical coupler, moving plate, and fixed plate. Both plates are attached with polymethyl methacrylate (PMMA) based polymer. The moveable and non-moveable capacitor plates are made of gold (Au), the mechanical coupler is made of Silicondioxide ( $\text{SiO}_2$ ), and the diaphragm is made of Au. The dielectric material of the sensor is taken as PMMA whose dielectric constant value is 3. The performance of TMCPS is examined using simulated PMMA polymers.

### SIMULATION OUTPUT

A pressure range of 0.1 MPa to 10.1 MPa with a step size of 1 MPa is employed as input pressures for the analysis. Figure 3 and 4 illustrates the simulated output deflection output of a sensor with 15  $\mu\text{m}$  and 20  $\mu\text{m}$  thicknesses at 10.1 MPa respectively.

As we see from the figures square diaphragm deflection occurs at the middle of the diaphragm. The output deflection of a sensor with a 15  $\mu\text{m}$  thick diaphragm is greater than that of a sensor with a 20  $\mu\text{m}$  thick diaphragm.

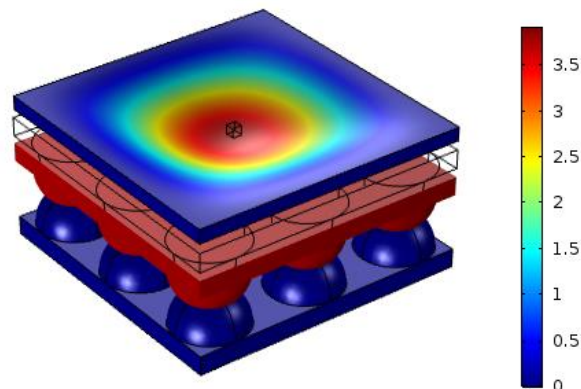


FIGURE 3

DISPLACEMENT OF SQUARE DIAPHRAGM WITH 15 $\mu\text{m}$  THICKNESS AT 10.1 MPa.

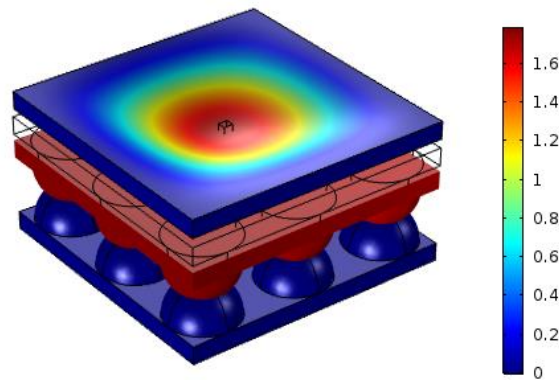


FIGURE 4

DISPLACEMENT OF SQUARE DIAPHRAGM WITH  $10\mu\text{m}$  THICKNESS AT 10.1 MPa.

### SIMULATED OUTPUT AND CALCULATED OUTPUT OF THE TMCPS

Table I lists the simulated and calculated displacement values for the proposed TMCPS. Deflection is also observed to increase as applied pressure is increased. The diaphragm displacement decreases as the thickness of the diaphragm increases. For the identical input pressures, the simulated and computed displacement values are quite near to each other.

TABLE I

SIMULATED VS CALCULATED DISPLACEMENTS FOR SQUARE DIAPHRAGM BASED TMCPS

Pressure (MPa)	15 $\mu\text{m}$ ( $\mu\text{m}$ )		20 $\mu\text{m}$ ( $\mu\text{m}$ )	
	Sim*	Cal**	Sim	Cal
0.1	0.0396	0.04085	0.01742	0.0186
1.1	0.4358	0.4849	0.19167	0.2046
2.1	0.8307	0.9258	0.3658	0.3906
3.1	1.2233	1.3666	0.5398	0.5766
4.1	1.6132	1.8075	0.7136	0.7625
5.1	1.9994	2.2483	0.8872	0.9485
6.1	2.3818	2.6892	1.0611	1.1345
7.1	2.7558	3.1300	1.2339	1.3205
8.1	3.1285	3.5709	1.4076	1.5065
9.1	3.4904	4.0117	1.5791	1.6924
<b>10.1</b>	<b>3.8514</b>	<b>4.4526</b>	<b>1.7516</b>	<b>1.8784</b>

\*Simulated value

\*\*Calculated value

Table II lists the capacitance values calculated and simulated for the proposed TMCPS. It can be seen from this data that the output capacitance is in the fF range. With an increase in applied pressure, the output capacitance values correspondingly rise.

TABLE II  
SIMULATED VS CALCULATED CAPACITANCE OF TMCPS.

Pressure (MPa)	PMMA 15 $\mu\text{m}$ (fF)		PMMA 20 $\mu\text{m}$ (fF)	
	Sim*	Cal**	Sim	Cal
0.1	17.1182	17.7673	17.1025	17.7623
1.1	17.2057	17.8548	17.1408	17.7991
2.1	17.2942	17.9432	17.1793	17.8360
3.1	17.3837	18.0324	17.2181	17.8731
4.1	17.4740	18.1226	17.2571	17.9103
5.1	17.5648	18.2136	17.2963	17.9477
6.1	17.6560	18.3056	17.3357	17.9853
7.1	17.7475	18.3985	17.3753	18.0230
8.1	17.8391	18.4923	17.4152	18.0609
9.1	17.9308	18.5871	17.4552	18.0989
<b>10.1</b>	<b>18.0223</b>	<b>18.6829</b>	<b>17.4954</b>	<b>18.1371</b>

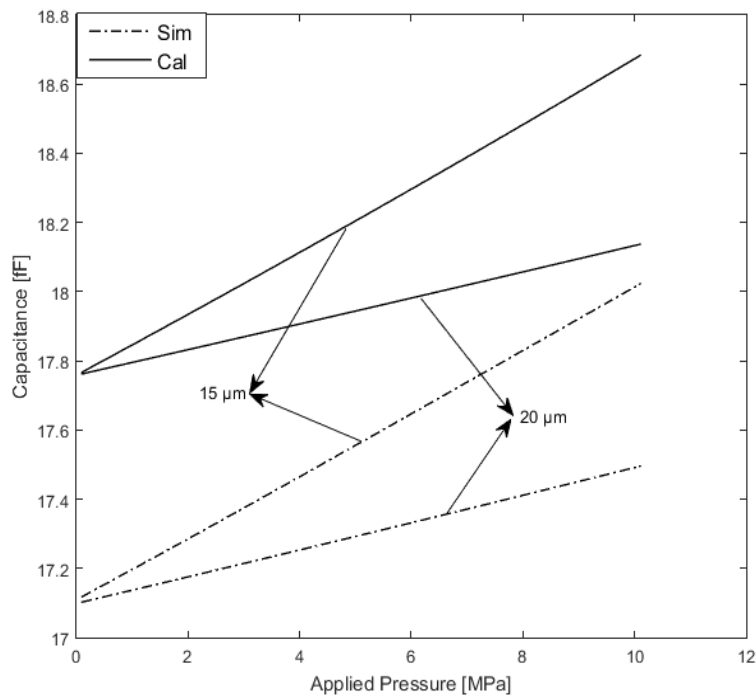


FIGURE 5

SIMULATED AND CALCULATED CAPACITANCE BASED ON PMMA SENSOR.

The PMMA-based TMCPS with a diaphragm thickness of 15  $\mu\text{m}$  offers the highest output values among the proposed types. Figure 5 depicts the simulated capacitance and calculated capacitance using a PMMA sensor. The sensor output capacitance is found to be very linear with the input pressure, which is a desirable property. It can also be shown that the calculated and simulated values are fairly similar. The output capacitance values are also linear with the input pressure, as shown in this diagram. The simulated output values are lower than the PMMA-based sensor's calculated output values.

## CONCLUSION

This research study focuses on the mathematical modelling and simulation of a TMCPS for sensing pressure ranges of 0.1 MPa to 10 MPa. PMMA is used to suggest and implement a design technique for a TMCPS. Because the simulated and calculated values are close to each other, the recommended design flow can be applied in the future.

Equations 7, 11, and 12 are validated with the COMSOL multiphysics simulator by comparing the mathematics calculated and simulated values. Because deflection is inversely related to diaphragm thickness, sensitivity improves when the diaphragm thickness is reduced. The sensitivity of the diaphragm rises as the length of the diaphragm increases because the length of the diaphragm is directly proportional to the length of the diaphragm.

Since the distance between the plates is inversely proportional to the sensor's sensitivity, decrease in the gap between the plates increase the sensitivity. Finally, by converting nonlinear deformation into linear displacement via a mechanical coupler, a sensor with a linear output characteristic is constructed.

For diaphragm thickness of 15  $\mu\text{m}$ , the sensitivity of the PMMA based touch mode capacitive pressure for simulated and calculated are 0.09 fF/MPa and 0.09 fF/MPa respectively.

## REFERENCES

- [1] D. Chen, Y. Cai and M. -C. Huang, "Customizable Pressure Sensor Array: Design and Evaluation," in *IEEE Sensors Journal*, vol. 18, no. 15, 1 Aug.1, 2018, pp. 6337-6344.
- [2] D. Alveringh, T. V. P. Schut, R. J. Wiegerink, W. Sparreboom and J. C. Lötters, "Resistive pressure sensors integrated with a coriolis mass flow sensor," *2017 19th International Conference on Solid-State Sensors, Actuators and Microsystems (TRANSDUCERS)*, 2017, pp. 1167-1170.
- [3] L. Shu, X. Tao and D. D. Feng, "A New Approach for Readout of Resistive Sensor Arrays for Wearable Electronic Applications," in *IEEE Sensors Journal*, vol. 15, no. 1, Jan. 2015, pp. 442-452.
- [4] D. P. J. Cotton, I. M. Graz and S. P. Lacour, "A Multifunctional Capacitive Sensor for Stretchable Electronic Skins," in *IEEE Sensors Journal*, vol. 9, no. 12, Dec. 2009, pp. 2008-2009.
- [5] Li Chen and M. Mehregany, "A Silicon Carbide Capacitive Pressure Sensor for High Temperature and Harsh Environment Applications," *TRANSDUCERS 2007 - 2007 International State Sensors, Actuators and Microsystems Conference*, 2007, pp. 2597-2600.
- [6] Run Wang, W. H. Ko and D. J. Young, "Silicon-carbide MESFET-based 400/spl deg/C MEMS sensing and data telemetry," in *IEEE Sensors Journal*, vol. 5, no. 6, Dec. 2005, pp. 1389-1394.
- [7] E. G. Bakhoun and M. H. M. Cheng, "High-Sensitivity Inductive Pressure Sensor," in *IEEE Transactions on Instrumentation and Measurement*, vol. 60, no. 8, Aug. 2011, pp. 2960-2966.
- [8] S. C. Bera, N. Mandal and R. Sarkar, "Study of a Pressure Transmitter Using an Improved Inductance Bridge Network and Bourdon Tube as Transducer," in *IEEE Transactions on Instrumentation and Measurement*, vol. 60, no. 4, April 2011, pp. 1453-1460.
- [9] C. Ghouila-Houri, Abdelkrim Talbi, Romain Viard, Quentin Gallas, Eric Garnier, Pascal Molton, Jérôme Delva, Alain Merlen, Philippe Pernod, "Robust thermal microstructure for designing flow sensors and pressure sensors," *2017 IEEE SENSORS*, 2017, pp. 1-3.
- [10] C. Ghouila-Houri, Abdelkrim Talbi, Romain Viard, Quentin Gallas, Eric Garnier, Pascal Molton, Jérôme Delva, Alain Merlen, Philippe Pernod, "MEMS high temperature gradient sensor for skin-friction measurements in highly turbulent flows," *2019 IEEE SENSORS*, 2019, pp. 1-4.
- [11] L. Li, L. -. Wang, L. Qin and Y. Lv, "The theoretical model of 1-3-2 piezocomposites," in *IEEE Transactions on Ultrasonics, Ferroelectrics, and Frequency Control*, vol. 56, no. 7, July 2009, pp. 1476-1482.

- [12] W. Yang, Q. Yang, R. Yan, W. Zhang, X. Yan, F. Gao, and W. Yan, “Dynamic Response of Pressure Sensor With Magnetic Liquids,” in *IEEE Transactions on Applied Superconductivity*, vol. 20, no. 3, June 2010, pp. 1860-1863.
- [13] Jiaqing Luo, Libing Zhang, Ting Wu, Haijun Song, Chengli Tang, “Flexible piezoelectric pressure sensor with high sensitivity for electronic skin using near-field electrohydrodynamic direct-writing method”, *Extreme Mechanics Letters*, Volume 48, 2021.
- [14] S. P. Timoshenko and S. Woinowsky-Krieger, “Theory of Plates and Shells”, *New York: McGraw Hill*, 1959. ISBN: 0070647798.
- [15] Ansel C. Ugural, “Plates and shells: theory and analysis”, Fourth edition, *Boca Raton, London, New York*, 2018. ISBN: 9781138032453.
- [16] Minhang Bao, “Analysis and Design Principles of MEMS Devices”, *Elsevier Science*, 2005, ISBN 978044451616.

#### AUTHOR INFORMATION

**Maibam Sanju Meetei**, Assistant Professor, Department of Electronics and Communication Engineering, Rajiv Gandhi University.

**Nabam Naga**, Student, Department of Electronics and Communication Engineering, Rajiv Gandhi University.

**Nyari Taji**, Student, Department of Electronics and Communication Engineering, Rajiv Gandhi University

**Rakesh Sharma, Student**, Department of Electronics and Communication Engineering, Rajiv Gandhi University.